

Design and Enhancement of Microstrip Patch Antenna Utilizing Mushroom Like-EBG for 5G Communications

Ahlam Alsudani¹ and Hamzah M. Marhoon^{2*}

¹Department of physics, College of Education for Pure Sciences Ibn Al-Haitham, University of Baghdad, Baghdad, Iraq; Email: ahlammajed2014@gmail.com¹

²Department of Forensic Sciences, Al-Esraa University College, Baghdad, Iraq

*Correspondence: hamzaalazawy33@yahoo.com

Abstract—Besides the considerable rise in wireless network usage and network-connected apps, this causes congestion, leading to a drop in data transmission speed. As a result of their high bandwidth availability and high data transfer speed, network operators recommended switching to higher frequencies. In communications via distance, the antenna plays a significant role in the transmission of the electrical radiated signal or the receiving of the electromagnetic signal. Many antennas can be utilized, one of which is the Microstrip Patch (MP) antenna. These antennas are very prevalent for their ease of configuration and design. On the other hand, it suffers from a lack of gain. In this research article, an MP antenna and MP antenna array are introduced and designed based on computer simulation technology antenna modelling software for 5G based-28 GHz applications. In order to optimise and enhance the simulated MP antenna parameters, the mushroom-like Electromagnetic Band Gap (EBG) is embedded with the MP antenna and MP antenna array to eliminate the presence of the surface waves that affecting negatively on the antenna gain. According to the simulation results, the gain is enhanced after utilising the mushroom-like EBG to be 6.48 dBi and significantly after applying the array configuration to be 11.9 dBi.

Keywords—5G, EBG, MP antenna, MP antenna array, CST

I. INTRODUCTION

Over recent past years, communication technology has undergone a number of evolutions. Whereas, the fastest-growing field of the communications industry among all communication techniques has been wireless communication. Perhaps it is accurate to declare that numerous impressive wireless communication improvements have been made in the area of mobile and cellular communications, that affect the users' daily lives in a direct manner. Due to the efficient shift in communication from the transmission of the voice toward the data transmission, the wireless communications concept has become more popular and obvious. From time to another, the utilization for the mobile applications, social media, and video broadcasting by the means of

portable internet-based devices has increased dramatically. Fig. 1 presents the congestion in data due to the utilization of the currently known applications [1, 2].

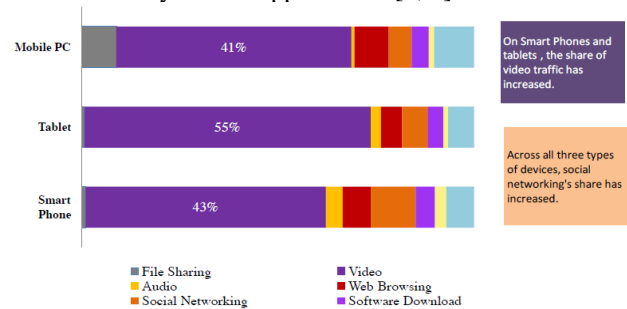


Figure 1. Volumes of mobile data currently tracked by application and device type.

So, the federal communications commission from time to another introduces the necessary rules to develop the mobile wireless network, Fig. 2 summarizes the evolution from 1G to 6G. Whereas, currently, the users' need for wireless networks with high data rates, lower latency, and greater energy efficiency has been continuously driven by this growth. Furthermore, it is clear that the need for mobile data traffic in the future will not be satisfied as the portion of the electromagnetic spectrum less the 20 GHz with promising communication features is nearly exhausted. As a result, an investigation has been focused on creating substitute technologies and making use of substitute spectrum allocations [3].

The 5G network is anticipated to especially increase communication capacity by utilizing a substantial portion of the millimetre wave (mm-wave) spectrum [4]. Additionally, it is anticipated to be able to deliver and sustain very high data rates up to 100 times faster than the 4G networks [5]. In order to satisfy the anticipated data rate and capacity, this results in a developed complicated network architecture. A number of fields, including pragmatic ultra-high definition, Artificial Intelligence, and Internet of Things applications are employed in the architecture for the savvy urban, intelligent transport, and smart grids all of the previously mentioned will be extremely improved thanks to the phenomenal increase in mobile data rates that are offered by the 5G technology.

Manuscript received November 7, 2022; revised December 12, 2022, accepted January 9, 2023.

Currently, the 5G are actually started and spread in many countries and the proposed frequencies used currently applied 28, 38, and 73 GHz bands that will be made unrestricted for future technologies as the mobile industry moves towards using the mm-wave spectrum [6]. Like these frequencies are affected extremely by the transmission loss such as the free space loss, the high oxygen absorption, and the requirements for line-of-sight communication. So that, the design of the antenna for such system should considered the mentioned limitations [7].

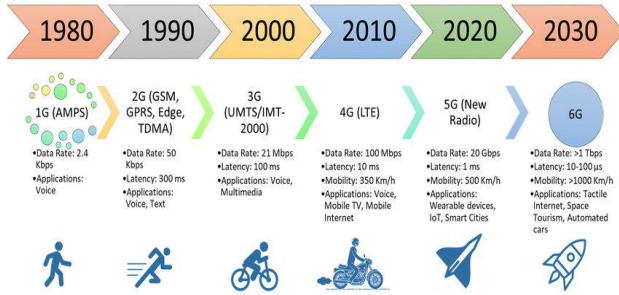


Figure 2. Development of wireless communications.

Because of the variety of the features such as the low profile, ease of design, low cost, and the planar structures that are characterised the Microstrip Patch (MP) antennas, thus, make such antennas are a proper candidate as well as a hot investigation topic for the 5G technology. Nonetheless, many of the weak points and drawbacks deform this type of antennas. The major issues of the MP antennas are the losses that are associated with the dielectric material and the presence of the surface waves [8]. On the basis of the previously reported issues, the MP antennas have small gain, tight bandwidth, and low efficiency [9]. Consequently, to minimize the drawbacks related to MP antennas many advancements and efficient improvement approaches can be applied which is summarized by the utilization of reconfigurable antennas [10], array antenna arrangement [11], metamaterials [12], frequency selective surfaces [13], engraved ground plane configuration [14], Electromagnetic Band Gap (EBG), and the multilayer antennas [15].

The researcher introduced many investigations and research articles regarding the performance enhancement of MP antennas in the literature. In [16] the authors have suggested a directional wideband MP antenna with a line-feeding and rectangular patch shape to support 5G transmissions at 28 GHz. The authors have begun with a basic rectangular MP antenna design and utilize a cutting-edge partial ground plane method to increase the introduced design performance and calibrate it to function in the range of 24 and 30 GHz. In this study, the researchers have been utilizing the Frequency Selective Surface (FSS) technique to optimize the W-shaped patch antenna performance parameters that are employed for the applications of 5G wireless communication systems. The suggested structure employs a Complementary Split Ring Resonator metamaterial and the FSS to improve gain, bandwidth, and reflection coefficient; the obtained values are 5.9 dBi at 5.5 GHz, -27.56 dB at 6 GHz, -12.65 dB at 4 GHz, and -21.24 dB at 8 GHz; an attractive radiation pattern is also created [17]. In this research article, the

researchers have been introduced an MP antenna from a ring patch shape with three resonances for the RF energy harvesting utilization. In order to optimise the total Bandwidth (BW) of the designed MP antenna the authors have etched a couple of complementary split-ring resonators at the patch. In addition, the authors introduced a cascade of circular mushroom electromagnetic bandgap structures (EBGs) with circular symmetry surrounding the antenna, increasing gain by 8.3 and 2 dB at 6.8 and 7.4 GHz, respectively [18].

In this research paper, we proposed a compact-sized rectangular MP antenna for 5G-based 28 GHz applications, which we enhanced by using an MP antenna array configuration. Then we added mushroom-like EBG cells to eliminate the presence of surface waves that spread across the antenna substrate and degrade its parameters. Finally, the obtained results are compared to demonstrate the ability of the array configuration and mushroom-like EBG to improve the MP antenna parameters.

The sections of the paper are systematised as follows: the second section describes the procedure for designing a typical MP antenna from a rectangular shape, the parametric calculations for antenna size, and the simulation operation inside the CST package. The third section interprets a general illustration regarding the mushroom-like EBG and embedding with the simulated standard MP antenna. The fourth section presents the enhancement process for the simulated antenna by applying the array configuration and embedding it with mushroom-like EBG structure to obtain the best performance. The fifth section comprises an illustration and interpretation of the acquired outcomes from the solver of the CST simulation package for the MP antenna and MP antenna array embedded with the mushroom-like EBG structure. Finally, the sixth section summarized the conclusion that was reached after developing this work.

II. PROPOSED ANTENNA DESIGN

Many of the main steps should be considered to construct the proposed MP antenna and MP antenna array, which are presented clearly in Fig. 3.

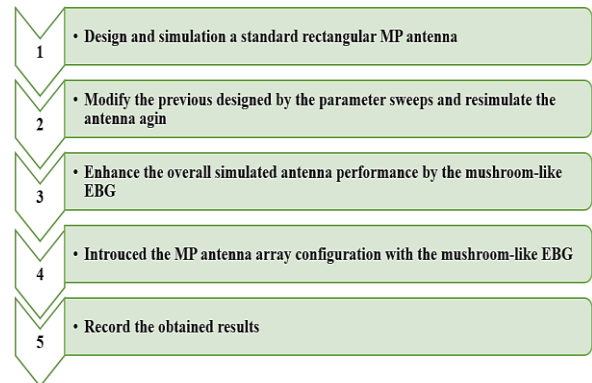


Figure 3. Procedure for the designed antenna.

According to the procedure in the previous Fig. 3, the first step in the design the standard MP antenna at an operation frequency of 28 GHz. This step is made by chosen the functional antenna parameters that are set in Table I.

TABLE I. SELECTED PARAMETERS FOR RECTANGULAR MP ANTENNA

Parameter	Explication
Operating frequency (f_o)	28 GHz
Dielectric Material	Rogers RO3003
Relative Permittivity	3
Thickness of Dielectric	0.130 mm
Input impedance	50 Ω

In accordance with the design procedure, the dimensions for the standard MP antenna should be assigned by applying a MATLAB program to evaluate the equations of the transmission line analysis mechanism that are listed below [19, 20]:

$$W_{Patch} = \frac{C_o}{2f_r\sqrt{0.5(\epsilon_r + 1)}} \quad (1)$$

$$\epsilon_{reff} = 0.5\{(\epsilon_r + 1) + (\epsilon_r - 1)\left[1 + 12\frac{t}{W_{Patch}}\right]^{-0.5}} \quad (2)$$

$$\Delta L = 0.412h \frac{(\epsilon_{reff} + 0.3)\left[\frac{W_{Patch}}{t} + 0.264\right]}{(\epsilon_{reff} - 0.258)\left[\frac{W_{Patch}}{t} + 0.8\right]} \quad (3)$$

$$L_{Patch} = \frac{C_o}{2f_r\sqrt{\epsilon_{reff}}} - 2\Delta L \quad (4)$$

where W_{Patch} is indicating to the patch width, ϵ_{reff} is indicating to the functional or the effective value for the permittivity, ΔL is indicating to the length extension because the presence of the fringing, t is indicating to the thickness of the dielectric material that utilized as an antenna substrate, the L_{Patch} is indicating to the patch length, and C_o is indicating to the light speed in the free space. The dimensions of the substrate and the ground plane are twice the length and width of the patch, respectively.

For the purpose of supplying the antenna with electrical power, there are several methods that can be applied for feeding as reported in [21], one of the most common methods and the easiest in the modelling is the strip line method. In this approach, a straight strip line is engraved on the same substrate and coupled with the edge of the antenna patch. In order to guarantee the extreme coupling between the antenna and the source of the power, the inset feed technology is utilized. In this manner, the strip line is inserted into the patch and small gaps on the sides of the feed are created, as shown in Fig. 4.

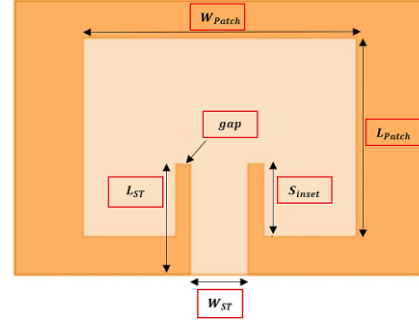


Figure 4. Structure of MP antenna with strip line.

In order to obtain dimensions for the strip line (i.e., the strip line length, width, inset distance, and gap) the set of the following equations is utilized [22, 23]:

$$W_{ST} = \frac{2t}{\pi} \left\{ \frac{377\pi}{2Z_o\sqrt{\epsilon_r}} - 1 - \ln\left(\frac{377\pi}{Z_o\sqrt{\epsilon_r}} - 1\right) + \frac{(\epsilon_r - 1)}{2\epsilon_r} \left[\ln\left(\frac{377\pi}{2Z_o\sqrt{\epsilon_r}} - 1\right) + 0.39 - \left(\frac{0.61}{\epsilon_r}\right) \right] \right\} \quad (5)$$

$$L_{ST} = 3.96 \times W_{ST} \quad (6)$$

$$g_{ST-P} = \frac{C_o \times 4.65 \times 10^{-9}}{f_r \sqrt{2\epsilon_{reff}}} \quad (7)$$

$$S_{inset} = \frac{\cos^{-1}\left(\sqrt{\frac{Z_o}{R_{in}}}\right)}{\frac{\pi}{L_{Patch}}} \quad (8)$$

where W_{ST} is indicating to the width of the strip line, Z_o is the equivalent resistance for the feed line which equals to 50 Ω , L_{ST} is indicating to the length of the strip line, g_{ST-P} is indicating to the gap among the strip line and the antenna patch, S_{inset} is indicating to how much the strip line inserted in the patch, and R_{in} is indicating to the impedance at the edge of the antenna patch.

The antenna simulation process initiates after this basic step, which includes calculating the antenna dimensions using the above-mentioned equations, Fig. 5 exemplifies the simulated standard MP antenna structure in the CST software package.

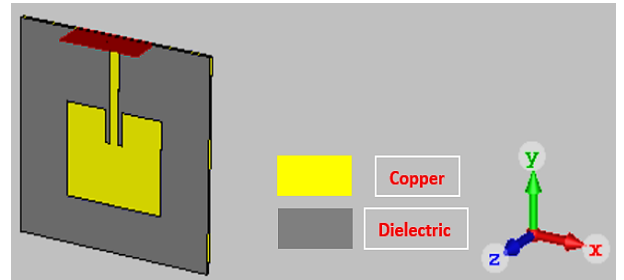


Figure 5. Standard MP antenna in CST package.

Based on the results obtained after conducting the simulation, it was remarked that the antenna suffers from the problem of impedance mismatch, and for the purpose of solving this problem, the method of adjusting the

antenna dimensions (i.e., sweep parameters) process is applied. This process is done by controlling the calculated antenna dimensions and re-stimulating the antenna in order to obtain the best results [24]. Table II exhibits the size of the antenna parameters before and after the adjusting process.

TABLE II. CALCULATED AND MODIFIED DIMENSIONS FOR THE RECTANGULAR MP ANTENNA

Parameter	Equations Value	Adjusted Value
Patch Width (W_{patch})	3.785 mm	3.62 mm
Patch Length (L_{patch})	3.048 mm	3.12 mm
Substrate Width ($W_{substrate}$)	7.570 mm	7.24 mm
Substrate Length ($L_{substrate}$)	6.096 mm	6.24 mm
Strip Line Width (W_{ST})	0.3315 mm	0.34 mm
Strip Line Length (L_{ST})	2.367 mm	2.3 mm
Strip Line Inset (S_{inset})	1.3127 mm	1.04 mm
Patch-Strip Separation Distance (g)	1.0206 mm	0.15 mm

III. MP ANTENNA WITH MUSHROOM-LIKE EBG

Once the MP antennas are powered with the electric signal the surface waves are spread over the face of the antenna dielectric substrate. These waves deteriorate the overall antenna parameters' such as antenna gain, efficiency, and BW which reflected negatively on the performance of the antenna [25]. Many of approaches can be utilized to eliminate the presence of the surface waves one of the most known approaches is the utilization of the mushroom-like EBG configuration [26]. In this method, a structure from a conductive material is printed on the same substrate and organized to be in the surrounding of the antenna patch. The EBG cells are joined directly with the aground plane by the means of the connectig vias. This configurations act as a passive filter to minimize or eliminate the effect of the surface waves [27], as shown in Fig. 6.

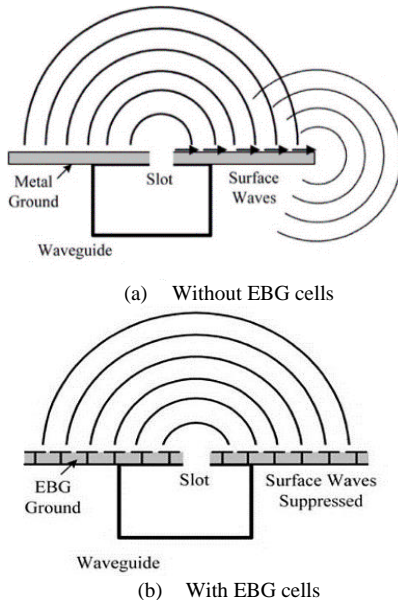


Figure 6. MP antenna with and without the EBG cells.

Commonly the EBG cells are represented as lumped elements with an inductor (L) and a capacitor (C), as exhibited in Fig. 7 so the EBG cells can be viewed as resonant LC. In the mathematical form the EBG cells can be modelled by utilizing the following equations [28, 29]:

$$C = \frac{W \epsilon_r (1 + \epsilon_r)}{\pi} \operatorname{sech}^{-1} \left(\frac{W + g}{W} \right) \quad (9)$$

$$L = 2 \times 10^{-7} h \left[\ln \left(\frac{2h}{r} \right) + 0.5 \left(\frac{2r}{h} \right) - 0.75 \right] \quad (10)$$

$$f_r = \frac{1}{6.28\sqrt{LC}} \quad (11)$$

where C is indicating to the corresponding capacitor to the EBG cells, L is indicating to the corresponding inductor to the EBG cells, W is indicating to the width of the EBG cell, g is indicatig to the spacing among the adjacent cells, h is indicating to the total height of the MP antenna, and r is indicating to the radius of the connecting via.

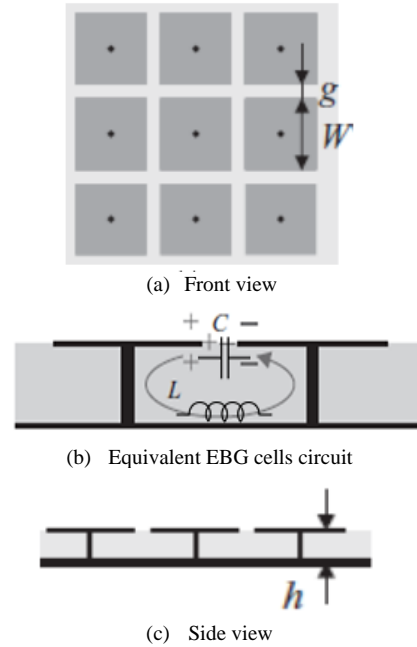


Figure 7. Organization of the mushroom-like EBG.

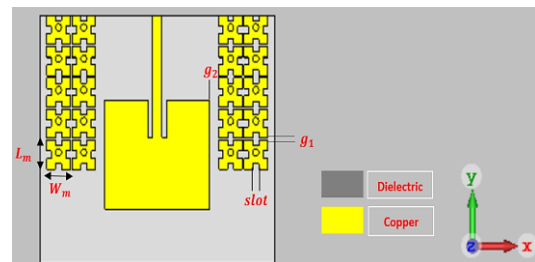


Figure 8. Proposed MP antenna with mushroom-like EBG elements.

The proposed MP antenna is loaded with 5×2 square-slotted EBG cells, as illustrated in Fig. 8. The dimensions

of the EBG cells, via radius, and the separation distance are demonstrated in Table III which are obtained after some modification according to the equations described in [30].

TABLE III. DIMENSIONS FOR THE MP ANTENNA WITH EBG CELLS

Parameter	Dimensions
Mushroom Cell Length (L_m)	0.80 mm
Mushroom Cell Width (W_m)	0.80 mm
Slots in the cell	$0.15 \times 0.20 \text{ mm}^2$
Adjacent Cells Spacing (g_1)	0.06 mm
Patch-Cell Spacing (g_2)	0.31 mm
Via Radius (r)	0.1 mm
Substrate Width ($W_{Substrate}$)	7.24 mm
Substrate Length ($L_{Substrate}$)	6.24 mm

IV. MP ANTENNA ARRAY WITH MUSHROOM-LIKE EBG

On the basis of the obtained outcomes from the CST software package, the MP antenna still has a low gain after adding the EBG elements. A 4×1 MP antenna array is introduced for the purpose of the overall parameters enhancement. To provide the best performance and impedance matching the parallel corporate feed technique is utilized. The principal step in the MP antenna array design is the design of the feeding network which is done by the means of the Antenna Magus[®] software. In this software, we just enter the operating frequency and the dielectric substrate characteristics then export the assembled structure to the CST package. Then the simulated previous single MP antenna is copied and coupled with strip feeding lines. Fig. 9 and Fig. 10, respectively, exhibit the feeding network with its dimensions after being exported to CST software and the completed MP antenna array structure.

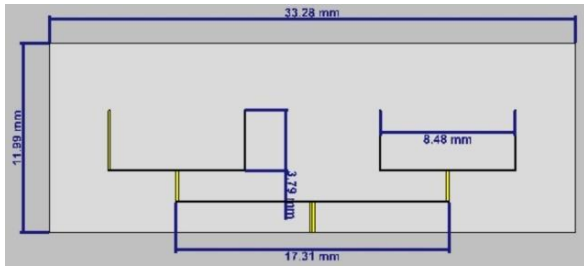


Figure 9. Corporate feed for the 1×4 array.

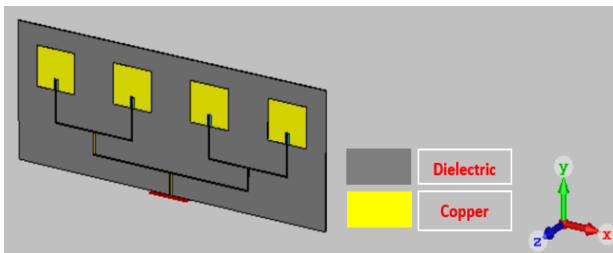


Figure 10. Simulated 4×1 rectangular MP antenna array.

Due to the presence of the feeding network and the adjacent element in the array configuration, the mutual coupling effect beside the surface waves will be present and affect the array performance. In order to minimize the mutual coupling effect and the surface waves in the same previous procedure, the mushroom-like EBG elements are

installed between the adjacent patches in the array. The mushroom-like EBG elements are allocated at a 3mm distance apart from the patch and 2 mm apart from the feeding network, as exhibited in Fig. 11.

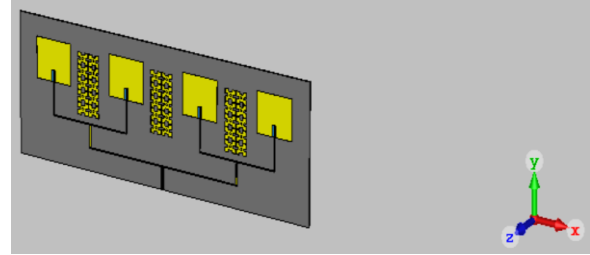


Figure 11. Proposed MP antenna array with mushroom-like EBG elements.

V. OBTAINED RESULTS

This section of the article exhibits the outcomes that are acquired by the means of the CST software solver for the MP antenna, MP antenna with mushroom-like EBG, MP antenna array, and MP antenna array with the mushroom-like EBG structure. The return loss (S_{11}) for the antennas is the measure of the degree of the mismatching between the antenna and the electric wave source, where it should be less or equal to -10 dB according to the previous studies which indicate that the antenna is received 90% of the total power that supplied by the means of the source and the rest has reflected the source. The S_{11} for the designed MP antennas before and after the optimisation (i.e., parameters modification) process are exhibited in Fig. 12.

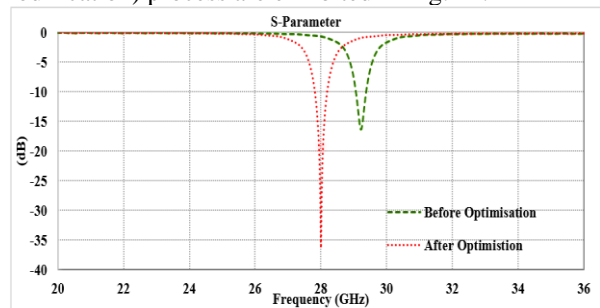


Figure 12. S_{11} results before and after optimisation.

As seen from the previous Fig. 12 the S_{11} results is enhanced and obtained as the required at $f_o=28$ GHz after the process of the parameters modification. Fig. 13 presents the S_{11} for the designed MP antenna and MP antenna array with the mushroom-like EBG.

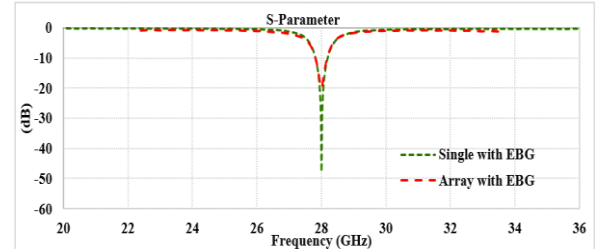


Figure 13. S_{11} results for the MP antenna and array with EBG cells

As seen from the previous Fig. 13 the S_{11} results for the single MP antenna design is enhanced after embedding with

the mushroom-like EBG. For the MP antenna array the due to the presence of the feeding network and the increase of the metalization loss S_{11} . It is possible to improve the S_{11} by adjusting the parameters according to the attempt that was made, but it was shown here that the antenna gain was affected. According to the previous studies, the MP antennas suffer from issues related to the substrate specifications (i.e., thickness and relative permittivity) that contribute to a poor gain [31]. Figures 14-17, respectively, exhibit the outcomes for the gain for the MP antenna after the modifications of the parameters, MP antenna with the EBG cells, MP antenna array, and MP antenna array with the EBG cells.

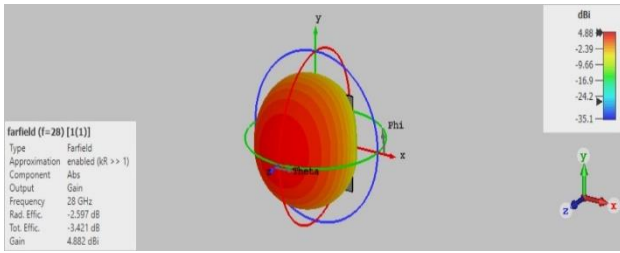


Figure 14. Optimized 3D gain pattern for the traditional MP antenna

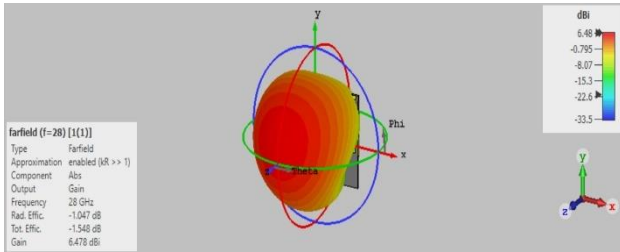


Figure 15. 3D gain pattern for the traditional MP antenna with EBG cells

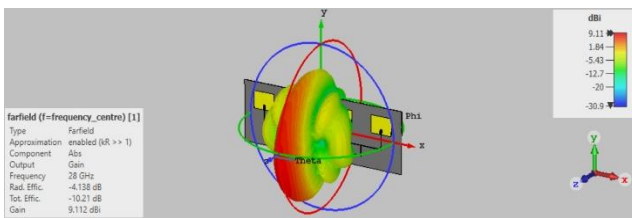


Figure 16. 3D gain pattern for the traditional MP antenna array.

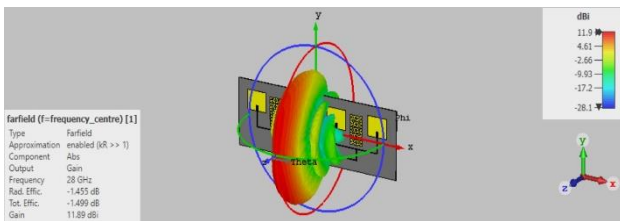


Figure 17. 3D gain pattern for the traditional MP antenna array with EBG cells.

As seen from the previously mentioned figures above the gain of the simulated antenna has been enhanced after utilising the mushroom-like EBG cells. The BW for the generic antenna is defined as the range of frequency bands in which the antenna parameters are roughly comparable to that calculated at the resonant frequency. In order to

summarise the results for the designed antennas Table IV is introduced.

TABLE IV. RESULTS SUMMARY FOR THE DESIGNED ANTENNAS

Parameter	Single MP antenna	Single MP antenna with EBG cells	MP antenna array	MP antenna array with EBG cells
S_{11} (dB)	-36.35	-47.7	-18.5	-20
BW (GHz)	0.381	0.482	0.603	0.804
Gain (dBi)	4.88	6.48	9.11	11.9

As presented in Table IV above the BW and the gain of the antenna are reinforced extremely when utilising the antenna array with the EBG.

VI. CONCLUSION

This research paper described a novel standard MP antenna embedding with a mushroom-like EBG based on the CST package for 5G mobile communications applications. A copper rectangular patch, a fully copper ground plane, and a Rogers RO3003 dielectric substrate were used to create the designed antenna. To reduce the spread of surface waves above the simulated MP antenna substrate, a new shape and arrangement of mushroom-like EBG cells have been printed on both sides of the simulated antenna patch, which contributes to improved antenna performance. The array configuration with parallel feeding and the mushroom-like EBG have been introduced to achieve maximum performance. The surface waves increase mutual coupling between array patches in the array configuration; by using EBG cells, this effect is reduced, and the performance of the MP antenna array is improved. The simulated antennas performed well, especially when the array structure was combined with EBG cells, whereas, a 11.9 dBi antenna gain has been reached.

CONFLICT OF INTEREST

The authors declare no conflict of interest.

AUTHOR CONTRIBUTIONS

As a joint scientific collaboration, the researchers carried out this work together. The work tasks were divided among the researchers, where the first researcher introduced the research plan and installed the mushroom cells with the antenna and with the array. After that, the second researcher carried out the simulation process with the CST and the optimization process. Finally, the researchers arranged the writing mechanism and compiled the paper. The authors agree that this is the last version of the paper.

REFERENCES

- [1] M. Z. Asghar, S. A. Memon, and J. Hämäläinen, "Evolution of wireless communication to 6G: Potential applications and research directions," *Sustainability*, vol. 14, no. 10, p. 6356, 2022.
- [2] S. Alraih, I. Shayea, M. Behjati, R. Nordin, N. F. Abdullah, A. Abu-Samah, and D. Nandi, "Revolution or evolution? technical

- requirements and considerations towards 6G mobile communications,” *Sensors*, vol. 22, no. 3, p. 762, 2022.
- [3] L. Chettri and R. Bera, “A comprehensive survey on Internet of Things (IoT) Toward 5G wireless systems,” *IEEE Internet of Things Journal*, vol. 7, no. 1, pp. 16-32, 2020.
- [4] N. Al-Falahy and O. Y. K. Alani, “Millimetre wave frequency band as a candidate spectrum for 5G network architecture: A survey,” *Physical Communication*, vol. 32, pp. 120-144, 2019.
- [5] D. Upadhyay, P. Tiwari, N. Mohd and B. Pant, “Capacity Enhancement for Cellular System using 5G Technology, mmWave and Higher order Sectorization,” in *Proc. IEEE 11th International Conference on Communication Systems and Network Technologies (CSNT)*, 2022, pp. 422-427.
- [6] N. Shabbir, L. Kütt, M. M. Alam, P. Roosipuu, M. Jawad, M. B. Qureshi, A. R. Ansari, and R. Nawaz, “Vision towards 5G: Comparison of radio propagation models for licensed and unlicensed indoor femtocell sensor networks,” *Physical Communication*, vol. 47, p. 101371, 2021.
- [7] R. Dangi, P. Lalwani, G. Choudhary, I. You, and G. Pau, “Study and investigation on 5G technology: A systematic review,” *Sensors*, vol. 22, no. 1, p. 26, 2021.
- [8] C. R. Storck and F. Duarte-Figueiredo, “A survey of 5G technology evolution, standards, and infrastructure associated with vehicle-to-everything communications by internet of vehicles,” *IEEE Access*, vol. 8, pp. 117593-117614, 2020.
- [9] I. Ahmad, W. Tan, Q. Ali, and H. Sun, “Latest Performance Improvement Strategies and techniques used in 5G antenna designing technology, a comprehensive study,” *Micromachines*, vol. 13, no. 5, p. 717, 2022.
- [10] H. M. Marhoon, N. Basil, H. A. Abdualnabi, and A. R. Ibrahim, “Simulation and optimization of rectangular microstrip patch antenna for mobile 5G communications,” *Jurnal Ilmiah Teknik Elektro Komputer dan Informatika (JITEKI)*, vol. 8, no. 2, pp. 249-255, 2022.
- [11] H. M. Marhoon and N. Qasem, “Simulation and optimization of tuneable microstrip patch antenna for fifth-generation applications based on graphene,” *International Journal of Electrical and Computer Engineering (IJECE)*, vol. 10, no. 5, pp. 5546-5558, 2020.
- [12] V. V. Yem and N. N. Lan, “Gain and bandwidth enhancement of array antenna using novel metamaterial structure,” *Journal of Communications*, vol. 13, no. 3, pp. 101-107, 2018.
- [13] N. Qasem and H. M. Marhoon, “Simulation and optimization of a tuneable rectangular microstrip patch antenna based on hybrid metal-graphene and FSS superstrate for fifth-generation applications,” *TELKOMNIKA (Telecommunication Computing Electronics and Control)*, vol. 18, no. 4, pp. 1719-1730, 2020.
- [14] N. A. Rao, V. V. Tallapragada, D. V. Reddy, and K. L. Prasad, “DGS loaded broadband circular patch antenna for satellite communications,” *Journal of Communications*, vol. 16, no. 11, pp. 485-491, 2021.
- [15] L. C. Paul, M. H. Ali, N. Sarker, M. Z. Mahmud, R. Azim and M. T. Islam, “A wideband rectangular microstrip patch antenna with partial ground plane for 5G applications,” in *Proc. Joint 10th International Conference on Informatics, Electronics & Vision (ICIEV) and 2021 5th International Conference on Imaging, Vision & Pattern Recognition (icIVPR)*, 2021, pp. 1-6.
- [16] A. B. Devarapalli and T. Moyra, “Design of a metamaterial loaded w-shaped patch antenna with FSS for improved bandwidth and gain,” *Silicon*, 2022.
- [17] S. R. Venkata, V. S. Sankar, and R. Kumari, “Patch antenna with multi-cell EBG for RF energy harvesting applications,” *International Journal of Microwave and Wireless Technologies*, pp. 1-9, 2022.
- [18] D. T. Tu, N. T. Phuong, P. D. Son, and V. V. Yem, “Improving characteristics of 28/38GHz MIMO antenna for 5G applications by using double-side EBG structure,” *Journal of Communications*, vol. 14, no. 1, pp. 1-8, 2019.
- [19] H. M. Marhoon, H. A. Abdalnabi, and Y. Y. Al-Aboosi, “Designing and analysing of a modified rectangular microstrip patch antenna for microwave applications,” *Journal of Communications*, vol. 17, no. 8, pp. 668-674, 2022.
- [20] H. Srivastava, A. Singh, A. Rajeev, and U. Tiwari, “Bandwidth and gain enhancement of rectangular microstrip patch antenna (RMPA) using slotted array technique,” *Wireless Personal Communications*, vol. 114, no. 1, pp. 699-709, 2020.
- [21] B. S. Taha, H. M. Marhoon, and A. A. Naser, “Simulating of RF energy harvesting micro-strip patch antenna over 2.45 GHz,” *International Journal of Engineering & Technology*, vol. 7, no. 4, pp. 5484-5488, 2018.
- [22] P. Elechi and P. O. Richard-John, “Improved multiband rectangular microstrip patch antenna for 5G application,” *Journal of Telecommunication, Electronic and Computer Engineering*, vol. 14, no. 2, pp. 7-14, 2022.
- [23] H. M. Marhoon, N. Qasem, N. B. Mohamad, and A. R. Ibrahim, “Design and simulation of a compact metal-graphene frequency reconfigurable microstrip patch antenna with FSS superstrate for 5G applications,” *International Journal on Engineering Applications (IREA)*, vol. 10, no. 3, pp. 193-201, 2022.
- [24] S. A. Alwazzan, A. A. Khamees, and M. Al-Rubaye, “Designing and simulating of tunable microstrip patch antenna for 5G communications utilising graphene material,” *Journal of Communications*, vol. 17, no. 4, pp. 280-286, 2022.
- [25] M. K. Mohsen, R. R. Jowad, and A. H. Mousa, “Performance of microstrip patch antenna for single and array element with and without EBG,” *Periodicals of Engineering and Natural Sciences (PEN)*, vol. 9, no. 3, pp. 22-28, 2021.
- [26] G. Li, *et al.*, “A novel approach to analyse the band gap of mushroom-like electromagnetic band gap structure,” in *Proc. Photonics & Electromagnetics Research Symposium (PIERS)*, 2022, pp. 391-396.
- [27] M. Ramzan, A. N. Barreto, and P. Sen, “Meta-surface Boosted Antenna to achieve higher than 50 dB TRX Isolation at 26 GHz for Joint Communication and Radar Sensing (JC&S),” in *Proc. 16th European Conference on Antennas and Propagation (EuCAP)*, 2022, pp. 1-5.
- [28] M. K. Abdulhameed, M. S. Isa, Z. Zakaria, I. M. Ibrahim, M. K. Mohsen, A. M. Dinar, and M. L. Attiah, “Novel design of triple-bands EBG,” *TELKOMNIKA (Telecommunication Computing Electronics and Control)*, vol. 17, no. 4, p. 1683, 2019.
- [29] S. Modak and T. Khan, “A slotted UWB-MIMO antenna with quadruple band-notch characteristics using mushroom EBG structure,” *AEU - International Journal of Electronics and Communications*, vol. 134, p. 153673, 2021.
- [30] M. K. Abdulhameed, M. S. Isa, I. M. Ibrahim, Z. Zakaria, M. K. Mohsen, M. L. Attiah, and A. M. Dinar, “Side lobe reduction in array antenna by using novel design of EBG,” *International Journal of Electrical and Computer Engineering (IJECE)*, vol. 10, no. 1, pp. 308-315, 2020.
- [31] A. Alsudani and H. M. Marhoon, “Performance enhancement of microstrip patch antenna based on FSS substrate for 5G communication applications,” *Journal of Communications*, vol. 17, no. 10, 2022.

Copyright © 2023 by the authors. This is an open access article distributed under the Creative Commons Attribution License ([CC BY-NC-ND 4.0](https://creativecommons.org/licenses/by-nc-nd/4.0/)), which permits use, distribution and reproduction in any medium, provided that the article is properly cited, the use is non-commercial and no modifications or adaptations are made.



Ahlam Alsudani received a B.Sc. degree in electrical engineering from the University of Baghdad/ Iraq, in 1992, and a master's degree in Electromechanical engineering /Electricity major from the University of Technology, Iraq in 2008. She is currently a Lecturer in the Department of Physics/ College of Education for Pure Science-Ibn Al Haitham/ University of Baghdad. Her current research interests include Communication Networks, Antennas, and Wireless Channels Modelling. She can be

contacted at email: ahlammajed2014@gmail.com.



Hamzah M. Marhoon was born in Baghdad, he received a B.Sc. degree in Electrical Engineering, from UOM in Baghdad, followed by an M.Sc. degree in Electronics and Communications Engineering from AAU in Amman. In 2022 he obtained a patent from The Central Agency for Standardization and Quality Control in Baghdad for the safety of LPG-based cars. He has many reviewing duties for reputed academic journals in the field of

Antennas, Microstrip Filters, IoT Systems, Embedded Systems, and Solar Energy.